Journal of magnetism and magnetic materials. 2013, vol. 345, p. 7-12. http://dx.doi.org/10.1016/j.jmmm.2013.05.047



# Intensity Distribution of Strong Magnetic Fields Created by Opposing Linear Halbach Assemblies of Permanent Magnets

**Václav Žežulka[1], Jaromír Pištora[2], Michal Lesňák[3*], Pavel Straka[1], Dalibor Ciprian[3], Jaroslav Foukal[3]**

[1]*Institute of Rock Structure and Mechanics, Academy of Sciences of the Czech Republic, v.v.i. V Holešovičkách 41, 182 09 Prague 8, Czech Republic*
[2]*Nanotechnology Centre, VSB – Technical University of Ostrava, 17. listopadu 15, 708 33 Ostrava-Poruba, Czech Republic*
[3]*Institute of Physics, VSB – Technical University of Ostrava, 17. listopadu 15, 708 33 Ostrava-Poruba, Czech Republic*

## Abstract

The work is devoted to a geometrical configuration of permanent magnets on the basis of opposing geometrically linear assemblies (e.g. Halbach arrays) for the generation of strong magnetic fields, which have been theoretically modeled and experimentally verified. The implementation of these opposing assemblies using NdFeB magnets of a total weight of 3.75 kg provided a value of magnetic flux density in the middle of an air gap of a width of 20 mm that was higher by 56% in comparison with the simplest possible design. When the air-gap width was 3 mm, the flux density reached a value of 2.16 T, which represents an increase of more than 100%. Simultaneously, however, unlike in the simplest possible parallel configuration, opposing Halbach assemblies have shown, in the middle of an air gap, a significant decrease of the magnetic flux density values when passing from the middle of the assemblies in the direction parallel to the x-axis.

Keywords: Magnetic field, Permanent magnets, Halbach arrays.

## Introduction

Numerous applications require the usage of magnetic fields with high values of magnetic flux density, or with an extreme gradient of this parameter. Thanks to their high values of remanent magnetization and energy density, permanent magnets on the basis of rare earths are predetermined for these purposes. In the 1970s, the first work concerning the so-called one-sided magnetic fluxes with planar magnetic geometries was published [1]. Subsequently, Halbach described a new quadrupole configuration using cobalt permanent magnets [2]. Marble claims [3] that through a relatively simple arrangement of permanent magnets it is possible to achieve more than 80% of the maximum possible magnetic field. The authors in the work [4] describe a geometric arrangement of NdFeB-type permanent magnets for magnetic resonance, which in the implemented device of a total weight of 790 kg (of which 290 kg is the weight of the NdFeB magnets from the material N42) generates, in an air gap of 0.06 m and a pole diameter of 0.2 m, a magnetic field of an induction of 1.6 T. In the same work, the authors mentioned that using the Halbach ring structure would make it possible to attain high fields and reduce the weight of the device, but this structure is too complicated to be manufactured and assembled.

With simplified Halbach cylinders, values of up to 1.8 T were attained [5]; with Halbach cylinders with iron pole magnetic-flux concentrators, the maximum level shifted to a value of 3.9 T [6]. The work [5] describes also an original source of a magnetic field on the basis of permanent magnets (Halbach sphere), where the calculated value of magnetic flux density in the central area (ø 6 mm x h 2.8 mm) exceeded the level of 4.3 T. Besides the size of the field generated, in many cases it is important to monitor the uniformity of this field as well. The solution to this problem has been discussed on the basis of Halbach geometrical configurations, i.e. ring dipole, square dipole and C-dipole [6]. At lower field values (below 0.4 $B_r$), the constructions of a C-dipole type are the most advantageous, whereas square and ring dipoles have been shown to be the best in the resolution of fields with high values of magnetic flux.

In systems with magnetic cooling, it is necessary to create some areas with a high and others with a low value of magnetic flux. The application of the Halbach cylinder, where some of the permanent magnets have been replaced by a magnetically soft material with a high value of relative permeability, can make it possible to achieve an almost 50% increase in the difference between the magnetic flux density values in the areas with high and low magnetic field levels [7].

Other publications have described constructions of autonomous sources of a strong magnetic field for magnetic separation chiefly in ceramic technological processes [8–10].

The aim of the work being presented is to build on these as well as mainly on other studies and knowledge concerning the simulation and implementation of strong magnetic fields [11–15]. It is devoted to the theoretical modeling, implementation and testing of a magnetic-field source based on the opposing linear Halbach assemblies of NdFeB magnets in comparison with the simplest possible design of the opposing permanent magnets from a material of the same type and quality.

## Model Formulation

The model of the setup can be formulated using a scalar magnetic potential. Two types of the sub-regions can be distinguished: source-free medium (air) and magnetic material (permanent magnets). Generally, magnetic induction is defined as:

$$B = \mu_0 M + \mu_0 H, \qquad (1)$$

where $H$ is the magnetic field intensity and $M$ is the magnetization. In our case, it is assumed that the magnetization in the permanent magnet is homogeneous and the medium is magnetically isotropic. The magnetic induction must satisfy the condition

$$\nabla \cdot B = 0. \qquad (2)$$

In order to compute the distribution of the magnetic field, the field will be expressed using a scalar magnetic potential defined as:

$$H = -\nabla\Phi. \qquad (3)$$

Inserting this expression for the scalar magnetic potential in (1) and combining the result with the divergence condition (2) leads to the following [16]:

$$\nabla \cdot \mu_0 \nabla\Phi = \nabla \cdot \mu_0 M. \qquad (4)$$

Equation (4) constitutes the formulation governing the scalar magnetic potential solution. Both types of the mentioned sub-regions are considered without free currents and the result is that the tangential components of the magnetic field intensity along their mutual boundaries are continuous.

However, the continuity of the normal components of the magnetic flux density must be enforced:

$$n_1 \cdot B_1 - n_2 \cdot B_2 = 0. \qquad (5)$$

Here index 1 refers to the permanent-magnet sub-region and index 2 is related to the adjacent air sub-region. This leads to the condition expressed as:

$$\mu_0 \;\; -\nabla\Phi_1 \;\; \cdot n + n \cdot \mu_0 M - \mu_0 \;\; -\nabla\Phi_2 \;\; \cdot n = 0, \qquad (6)$$

where $n$ is the normal unit vector on the interface boundary printing from sub-region 1 to sub-region 2. Equation (4) can be treated as governing the differential equation on the domain:

$$L\Phi = f \qquad (7)$$

and together with the appropriate boundary condition it defines a boundary-value problem for the scalar magnetic potential Φ. The solution to this problem can be obtained using the finite element method (FEM). Here, $L$ is the differential operator and $f$ is the so-called excitation or forcing function. The solution to the boundary-value problem can be formulated using a variational approach [16]. Instead of solving Equation (7) directly, a functional minimization on the domain Ω is used. The functional can be written as:

$$F \;\; \Phi \;\; = \;\; _{\Omega} \; \nabla \cdot \mu_0 \nabla \Phi - \mu_0 \nabla \cdot M d\Omega = 0, \qquad (8)$$

where Φ is an approximate solution to (7). An approximation of the unknown solution in the $e$-th element can be expressed as:

$$\Phi^e = \;\; {}^{n}_{j=1} N_j^e \Phi_j^e = \;\; N_j^e \;\; ^T \;\; \Phi^e \;\; = \;\; \Phi^e \;\; ^T \; \mathrm{N}^e \;\; . \qquad (9)$$

$n$ denotes the number of nodes in the element, $\Phi_j^e$ is the value of the magnetic potential at the $j$-th node and $N_j^e$ is the interpolation function for that node. When the approximate solution is inserted in (8) and the Galerkin's method is followed with the choice of the weighting functions being the same as the functions for the expansion of the approximate solution, the minimization procedure leads to the linear equation systems:

$$ {}^{M}_{e=1} \;\; K^e \;\; \Phi^e \;\; - \;\; b^e \;\; = 0 \, , \qquad (10)$$

where the matrices $K^e$ and $b^e$ for each element are obtained using (8), and where $\Phi^e$ denotes the column vector of the scalar magnetic potential values for the nodes of the $e$-th element. The summation over $e$ is related to the total numbers of elements in the domain. Once the system of the elemental equation is assembled, the values of the scalar magnetic potential in the domain can be computed. On the basis of Equations (8) – (10), the course of the values of magnetic induction in the middle of the gap between two opposing Halbach arrays was computed (see Figs. 7 and 8).

The numerical modeling of the experimental array by FEM was carried out using the ANSYS software package. Each system of Halbach assemblies was represented by appropriate 3D model in order to obtain the magnetic flux distribution in the air gap. The magnetic assemblies were surrounded by a rectangular air region with the infinite elements on its outer boundary to simulate the infinite domain. The geometric dimensions of the mentioned region were given by the distances from outer model boundaries to the appropriate magnetic assembly surfaces. The distances were chosen as multiples of magnetic assemblies dimensions in x and z-directions, and y-size plus half-gap thickness in y-direction (see the figures 2-4). The value of the multiple varies from 5 to 7. Such conditions were checked to secure stable results of the computation. From the same reason, the size and the number of the elements in the model was tested as well. It was found that in order to achieve stable results, models had to contain approximately 2 500 000 elements. Further increase of element number does not substantially improve the stability increase, and moreover it leads to the superfluous growth of the computational time.

## Experimental

The proposed method of strong magnetic field generation is directly based on the results and knowledge acquired during previous work with real permanent magnet arrays. In the paper [11] are described the chosen types of separate assemblies of magnets including method of determining their dimensions and measured values of stray magnetic field. Such types (material, geometry) of separate magnet assemblies were selected in our configurations that could be compared with the magnet designs described by Marble [3] in Figs 6(a) and 6(b). In mentioned paper [3] Marble derives a magnetization pattern leading to the strongest possible stray field at a remote point. For this reason, the dimensions of these realized separate assemblies were designed so as to preserve the same dimensional ratios evident in Fig. 3(a) [3]. For width of the inner block in the Halbach array leading to the mentioned strongest magnetic field, Marble reports [3, page 579] the value 0.154 units. In our magnet arrangements we generally apply the different dimensions of permanent magnet blocks in the Halbach arrays. This approach has been used for example in [19].

The original simple device [11, Fig.4] designed for placing of individual magnetic blocks into assemblies was further modified and doubled in order to be able to create two opposing magnetic arrays with a continuously adjustable mutual distance. The new assembling tool depicted in Figure 1 allows set the distance between the arrays (air gap width w) in the range from 3 to 160 mm by moving the top array with respect to the fixed bottom one. Magnetic flux density in the center of the air gap is then measured as the function of increasing gap width. When the gap width is fixed, magnetic flux density distribution along the axis of the gap can be measured as well.

Fig. 1 Device for placing NdFeB magnets into two opposing assemblies

As the basis, NdFeB blocks with sizes of 50 x 50 x 30 mm from the N45 material with remanence Br = 1.354 T and maximum energy product $(BH)_{max}$ = 348 kJ/m$^3$ were used. Because it was not possible to meet the required dimensions of Halbach array using the mentioned blocks only, some smaller blocks has to be formed by cutting the larger one in such a way that the preferential orientation of the demanded magnetization direction was preserved. Thus the Halbach arrays in Figures 2, 3 and 4 depict the magnets as they are really assembled. As to the used model formulation, ideal conditions considering homogeneously magnetized blocks with magnetization parallel to the block faces were assumed. From this point of view, the neighboring blocks are considered as one domain, provided that their magnetization vectors are parallel. For example the upper (lower) array depicted in Figure 2 is treated as one continuous domain despite the fact that it consists of four pieces. According to the principles of Halbach array formation, the magnet assemblies are configured in such a way that the effect of one-sided magnetic flux creates a strong magnetic field in the air gap. The measurements of the magnetic flux density in the individual configurations were performed using F. W. Bell teslameter, type 5080 with the Hall transverse probe. The value of magnetic flux density was always measured in the gap center and this point corresponds to the coordinate system origin in Figures 2, 3 and 4.

*Permanent-Magnet Assembly Configuration*

During the measurements of the dependences of magnetic flux density in the case of the opposing assemblies, the beginning of the coordinates x and y (point 0) was always selected in the middle of the surface of the bottom array as depicted in Figures 2, 3 and 4. It must be underlined that these Figures do not display any magnet designs, but actually realized magnet assemblies where precision cuts and a way of assembly can influence the measured values of magnetic flux density. Therefore, for the possibility of eventual further comparison and impact assessment the proportions are plotted in Figures, including inner lines, and displayed, and so are all individual magnets from which the assemblies are composed.

a) *Assemblies 1 and 1´*

This arrangement (the simplest possible design of the opposing magnets) is schematically depicted in two views including the dimensions in Fig 2. First, the dependence of the magnetic flux density in the middle of an air gap $B_{yw/2}$ on the width of this gap $y_w$ with $y_w$ ranging from 160 mm to 3 mm was measured. This dependence is depicted in Fig. 5 (blue curve, diamonds). Furthermore, the dependence of the magnetic flux density $B_{yw10}$ in the middle of an air gap of the constant width $y_w$ = 20 mm (on the level of $y_w/2$ = const. = 10 mm) on the parameter *x* (x-axis is parallel to the surface of the permanent magnets – Fig. 2) was determined to be in the range of *x* from -35 to +35 mm. The measured dependence is illustrated in Figure 6 (blue curve, diamonds).

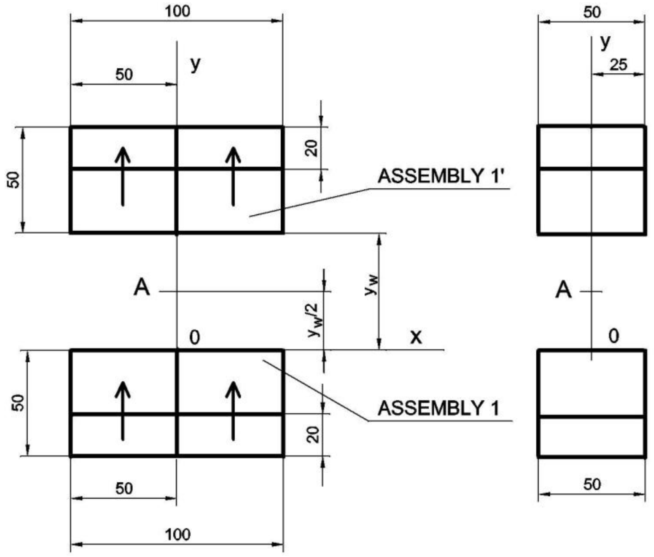


Fig. 2 Schematic picture of opposing assemblies 1 and 1´

b) *Assemblies 2 and 1´*

The arrangement (a Halbach array/assembly with the opposing simplest assembly of magnets) is represented in Fig. 3. The measurement was performed similarly as in the previous case; the measured dependence $B_{yw/2} = f(y_w)$ is plotted in Fig. 5 (red curve, squares), the dependence $B_{yw10} = f(x)$ in Fig. 6 (red curve, squares).

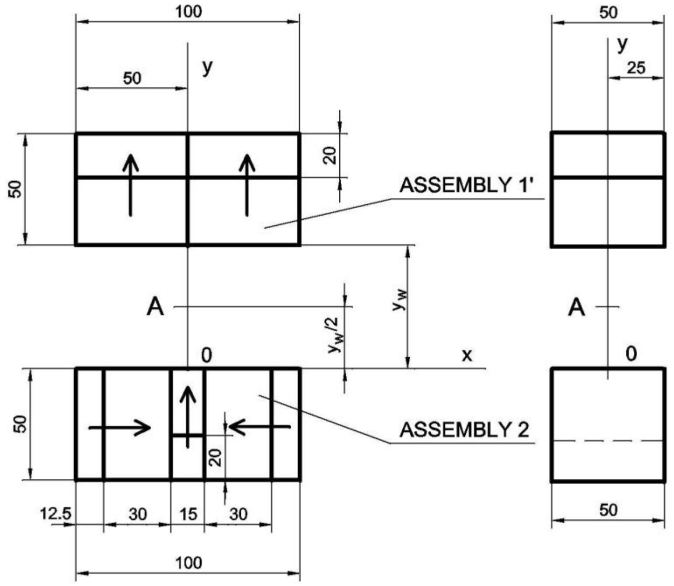


Fig. 3 Schematic picture of opposing assemblies 2 and 1´

c) *Assemblies 2 and 2´*

This arrangement (two opposing Halbach arrays) is depicted in Fig. 4. The measurement was performed again in the same way as the previous one; the respective dependences are likewise plotted in Figs. 5 and 6 (green curves, triangles).

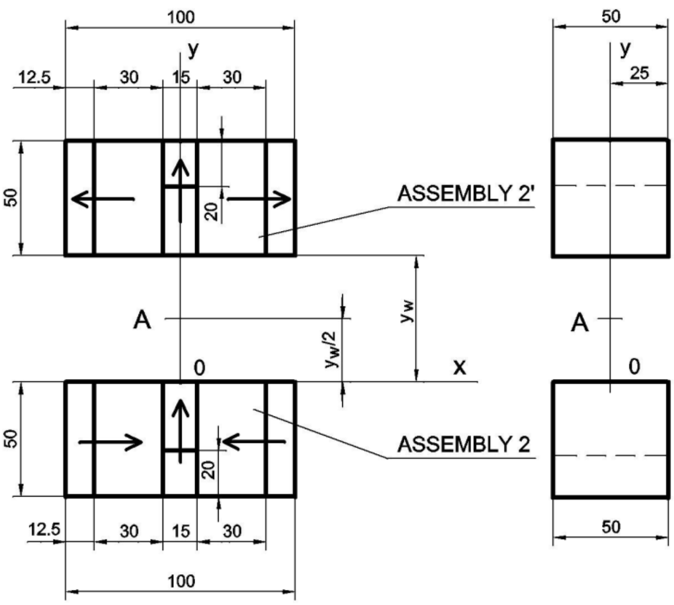


Fig. 4 Schematic picture of opposing assemblies 2 and 2´

## Theoretical and Experimental Results

The measurement of the magnetic flux density as a function of the air gap width with all of the arrangements above has provided the dependences declared in Fig. 5.

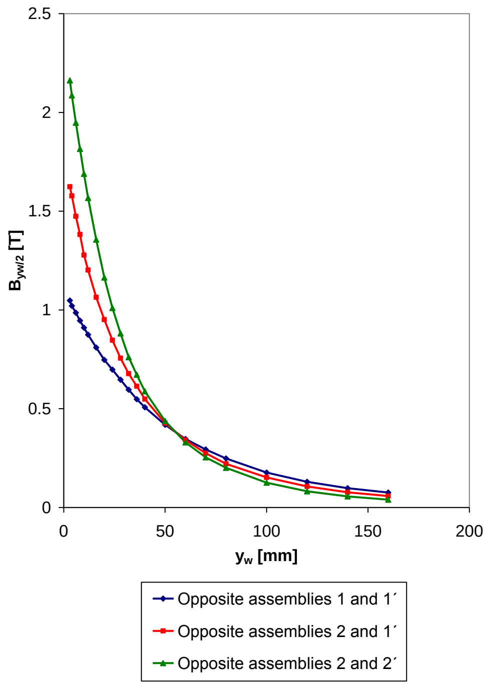


Fig. 5 The dependences $B_{yw/2} = f(y_w)$ with the opposing three types of magnet assemblies

The measurement of the magnetic flux density in the middle of an air gap of constant width as a function of the parameter *x* with all of the above-mentioned arrangements has provided the dependences depicted in Fig. 6.

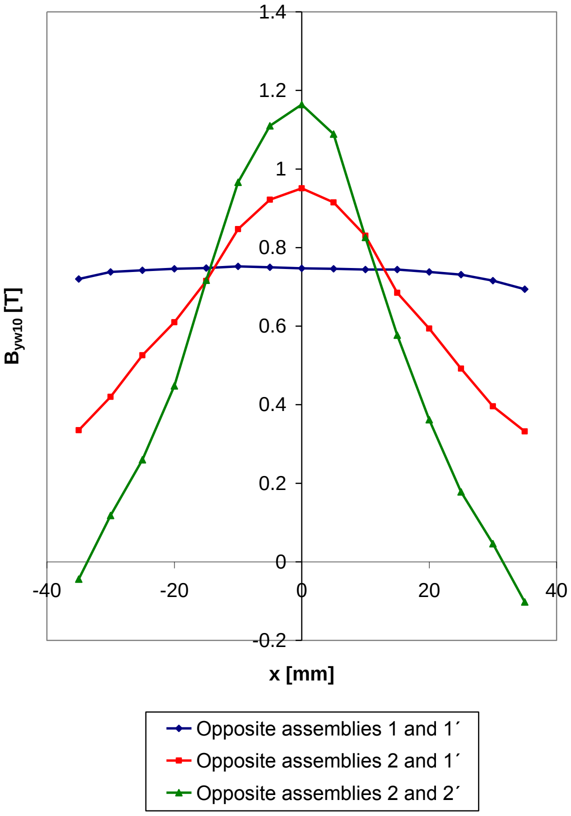


Fig. 6 The dependences $B_{yw10}$ = f(x) with the opposing assemblies for $y_w$ = const. = 20 mm

A comparison of the values of the magnetic flux density $B_{yw/2}$ obtained through the modeling (Equations (8)–(10)) and measurement with the arrangement implemented (see Fig. 4) is clear from Fig. 7.

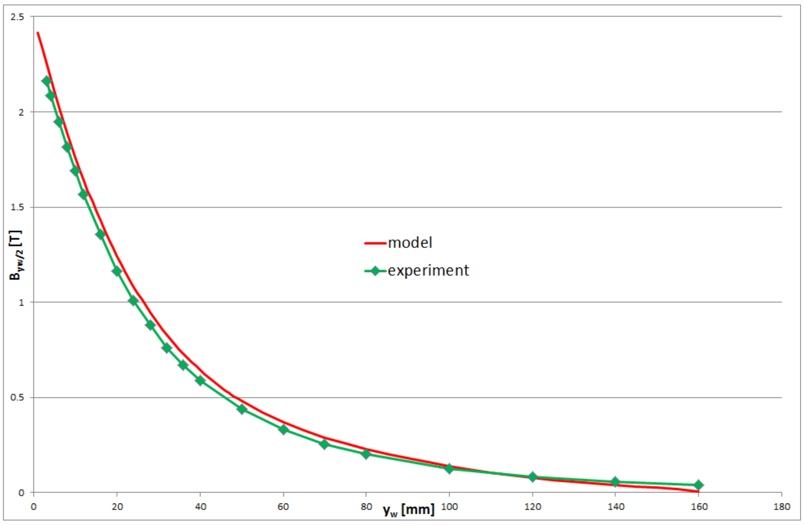


Fig. 7 Comparison of the course of the values of the magnetic flux density in the middle of an air gap between two opposing linear Halbach assemblies – model and experiment

A comparison of the values of the magnetic flux density $B_{yw10}$ obtained through the modeling (Equations (8)–(10)) and measurement with the arrangements implemented (see Fig. 6) is clear from Fig. 8.

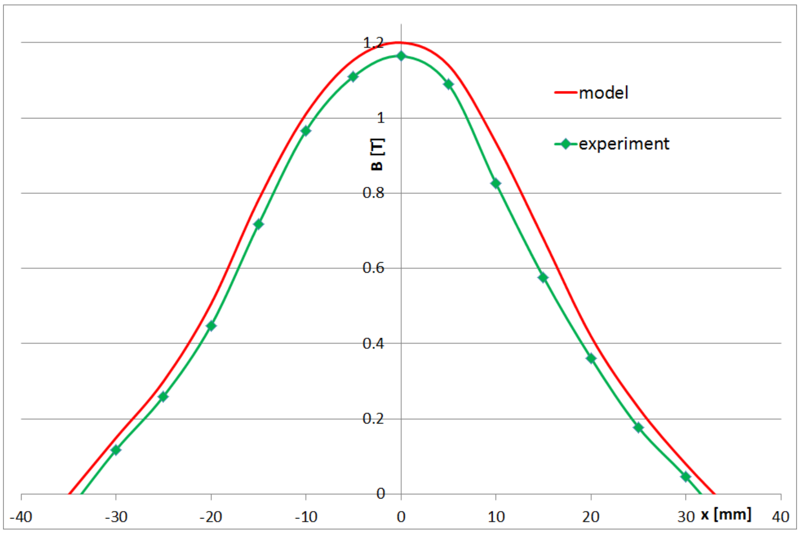


Fig. 8 Comparison of the distribution of the magnetic field in the middle of the air gap along x- axis – model and experiment

## Discussion

A comparison of theoretical results, acquired through modeling, and experimental results indicates their high correlation. In the case of two opposing linear Halbach arrays, the agreement is within 5% (Fig. 7).

In the case of the opposing parallel magnet arrays (NdFeB magnets, N45 type, $B_r$ = 1.354 T) in the simplest arrangement (Fig. 2) with a gap width of 20 mm, a magnetic flux density value of 0.747 T was measured in the middle of this gap (Fig. 5). If one assembly of this arrangement is replaced by a Halbach configuration (Fig. 3), the magnetic flux density value shifts to the level of 0.951 T (Fig. 5). The geometry of two opposing Halbach assemblies moves this value to 1.164 T (Fig. 5). It can thus be stated that the usage of this arrangement (Fig. 4) has led to an increase in the value of magnetic flux density, in the middle of a gap of a width of 20 mm, by approximately 56% in comparison with the simplest arrangement. When the width of the gap was reduced to 3 mm (when the aforementioned device (Fig. 1) is utilized, it is the minimal distance between the opposing assemblies), when the magnetic flux density values 1.048 T and 2.162 T were similarly measured, the increase in the magnetic flux density was even more significant and reached as much as 106%. As arises from Fig. 5, this gradual, significantly increasing difference in the magnetic flux density in favor of the arrangement with the opposing Halbach assemblies occurs in the given case when the air gap is gradually reduced approximately from 60 mm. When the gap width was increased above this value, a slightly higher magnetic flux density was, on the other hand, measured in the case of the simplest arrangement.

It needs to be emphasized that the above-mentioned significant increase in magnetic flux density was achieved by the configuration when the ideal Halbach geometry [17, Fig. 1 a)] was modified by assembling three permanent magnets (Fig. 4). In the aforementioned specific case of the implementation of two opposing Halbach assemblies, the values of magnetic flux density in the air gap of the width up to 5 mm were higher than 2 T. This result was made possible by assembly and size modification of essentially only a few NdFeB magnets, currently commonly available in terms of both the initial dimensions and the quality of the material. The total weight of the magnets in both opposing arrays together is only 3.75 kg. As was already said in the introduction in connection with the very complicated manufacture and assembly of the ring Halbach array [4], not even the ideal Halbach arrangement is easy to implement technically [18]. Nevertheless, the implementation of the opposing linear Halbach arrays/assemblies, described in the text above, has been shown to be relatively feasible.

With the usage of trapezoidal magnets (a series of three permanent magnets) in the Halbach configuration, it is possible to expect a further strengthening of the field by 3–5% [3].

An important issue is the homogeneity of the field along the direction of the x-axis. Fig. 6 captures this situation again at a gap width of 20 mm on the line in the middle of this gap. As arises from the physical principles with the simplest configuration (Fig. 2), the magnetic flux density value is almost constant. On the contrary, in the case of opposing Halbach assemblies, we have observed a decrease of the maximum magnetic flux density value in the direction of x-axis at a distance of ±20 mm from the middle of the assemblies by up to 50%. This decrease further increases with the growing distance x from the middle of the assemblies. Also the proposed theoretical model for the description of the longitudinal distribution of the field is in agreement with this course of magnetic flux density (Fig. 8).

The question is the dependence of the results on the dimensions of the magnet blocks. The permanent magnet sets with half and double the thickness of magnetic blocks (in comparison with Fig. 3) have been modeled. For double thickness the maximum value of 1.45 T has been achieved (the others parameters are the same as in Fig. 3), for half thickness the maximum value of magnetic field is 0.94 T. In the direction of the x–axis at a distance of ± 20 mm from the middle of the assemblies the decrease from 50% (for double geometry) up to 20% (for half thickness) is observed.

If the length of the array permanent magnets components is twice as long (scaling in x – direction, dimensions in y – direction are fixed) in comparison with original arrangement (see Fig. 3) the maximum value of magnetic field in the middle of the 20 mm gap has been specified to be 1.05 T. In the direction of the x–axis at a distance of ±20 mm from the middle of the assemblies the decrease of 30% is observed. For the distance ± 15 mm (x - direction) the value 1.05 T is practically constant. If the length of the array is half as long in comparison with original arrangement (see Fig. 3), the important end effects have been observed. In this case in the x-axis direction in the interval (±15 mm, ±20 mm) from the middle of the assemblies we observe antiparallel orientation of magnetic flux density vector. For distance more ±20 mm the magnetic flux density vector orientation is changed to the original direction.

## Conclusions

Geometrical configurations of permanent magnets on the basis of Halbach assemblies for the generation of strong magnetic fields have been proposed, and the respective distributions of the implemented magnetic fields have been theoretically modeled and experimentally verified. A comparison of the results of the model approaches and experiments has shown that using current software products it is objective to find a high correlation between theoretical and experimental results.

Both the computer simulation and the implementation have confirmed that by means of the mentioned opposing linear Halbach assemblies equipped with NdFeB magnets with a high energy product, it is possible to achieve in the defined volume magnetic fields with magnetic flux density values exceeding the level of the remanent magnetization of the permanent magnets used. The application of permanent magnets of larger sizes (or magnetic blocks from the same material) thus opens a real possibility for the creation of a strong magnetic field in a greater volume for various applications.

## Acknowledgment

This work has been supported by the Research Program for the years 2012–2017, Institute of Rock Structure and Mechanics, Academy of Sciences of the Czech Republic, v.v.i., (#USMH-130/135/2011) and by the Czech Science Foundation (#P205/ 11/2137).

## References

[1] J. C. Mallinson, One-Sided Fluxes – A Magnetic Curiosity?, IEEE Transactions on Magnetics 9 (1973) 678.
[2] K. Halbach, Strong Rare Earth Cobalt Quadrupoles, IEEE Transactions on Nuclear Science NS-26 (1979) 3882.
[3] A. E. Marble, Strong, Stray Static Magnetic Fields, IEEE Transactions on Magnetics 44 (2008) 576.
[4] Z. Wang, W. H. Yang, X. B. Zhang, L. L. Hu and H. X. Wang, A Design of 1.5 T Permanent Magnet for MR Molecular Imaging, IEEE Transactions on Applied Superconductors 20 (2010) 777.
[5] F. Bloch, O. Cugat, G. Meunier, J. C. Toussaint, Innovating approaches to the generation of intense magnetic fields: Design and optimization of a 4 Tesla permanent magnet, IEEE Transactions on Magnetics 34 (1998) 2465.
[6] Ch. Li and M. Devine, Efficiency of permanent magnet assemblies for MRI devices, IEEE Transactions on Magnetics 41 (2005) 3835.
[7] R. Bjørk, C. R. H. Bahl, A. Smith, N. Pryds, Improving magnet designs with high and low field regions, IEEE Transactions on Magnetics 47 (2011) 1687.
[8] V. Žežulka, P. Straka, A new method of assembling large magnetic blocks from permanent NdFeB magnets, Acta Geodynamica et Geomaterialia 4 (2007) 75.
[9] V. Žežulka, P. Straka, Methods of assembling large magnetic blocks from NdFeB magnets with a high value of $(BH)_{max}$ and their influence on the magnetic induction reached in an air gap of a magnetic circuit, IEEE Transactions on Magnetics 44 (2008) 485.
[10] V. Žežulka, Magnetic circuit with large blocks from NdFeB magnets for suspended magnetic separators, Acta Geodynamica et Geomaterialia 7 (2010) 227.
[11] V. Žežulka and P. Straka, The realization of strong, stray static magnetic fields, Acta Geodynamica et Geomaterialia 9 (2012) 71.
[12] R. Bjork, A. Smith, C.R.H. Bahl, Analysis of the magnetic field, force, and torque for two-dimensional Halbach cylinders, Journal of Magnetism and Magnetic Materials 322 (2010) 133.
[13] A. Sarwar, A. Nemirovski, B. Shapiro, Optimal Halbach permanent magnet designs for maximally pulling and pushing nanoparticles, Journal of Magnetism and Magnetic Materials 324 (2012) 742.
[14] J.E. Hilton, S.M. McMurry, An adjustable linear Halbach array, Journal of Magnetism and Magnetic Materials 324 (2012) 2051.
[15] R. Bjork, C.R.H. Bahl, A. Smith, N. Pryds, Comparison of adjustable permanent magnetic field sources, Journal of Magnetism and Magnetic Materials 322 (2010) 3664.
[16] J. Jin, The Finite Element Method in Electromagnetics, J. Wiley & Sons Inc., New York, 2002.
[17] Z. Long, G. He, S. Xue, Study of EDS & EMS Hybrid Suspension System with Permanent-Magnet Halbach Array, IEEE Transactions on Magnetics 47 (2011) 4717.
[18] J. Choi, J. Yoo, Design of a Halbach magnet array based on optimization techniques, IEEE Transactions on Magnetics 44 (2008) 2361.
[19] K. J. Meesen, B. L. J. Gysen, J. J. H. Paulides, E. A. Lomonova, Halbach Permanent Magnet Shape Selection for Slotless Tubular Actuators, IEEE Transactions on Magnetics 44 (2008) 4305.